F. H. Mitchell, Jr. W. R. Mahaffey R. F. Jacob

Modeling Plasma Effects on Radar Cross Section of Reentry Vehicles*

Abstract: In order to design a radar to detect, track, and identify unknown targets, models of the expected electromagnetic scattering properties of the targets must be developed. This communication begins with a qualitative discussion of interactions between an incident wave and a plasma-clad body in order to give the general reader a heuristic understanding of the problem background. Then rigorous calculations of normalized backscatter cross section for a spherical, plasma-clad body, and the limitations of this model, are presented in context with earlier background material.

A plasma simulation technique is described as a means for modeling a diverse range of reentry bodies and plasmas that are not amenable to analytic solution. The theoretical analysis can be used to validate the simulation technique in a spherical configuration after which the technique can be used to simulate many other plasma shapes around a variety of bodies.

I. Introduction

In order to design a radar to detect, track and identify unknown targets, models of the expected electromagnetic scattering properties of the targets must be developed. (The magnitude and phase of the received signal and its time and angular variations are all functions of target parameters.) The scattering properties of a given body are usually described by its cross section $\sigma(\theta_0, \Delta\theta)$ which represents the effective area of the target for scattering through an angle $\Delta\theta$ energy from a wave incident at angle θ_0 . For a single radar acting as both transmitter and receiver, only the backscatter cross section $\sigma(\theta_0, \Delta\theta = \pi) = \sigma_B(\theta_0)$ is measured.

For a few simple bodies σ_B can be calculated theoretically, and for more complex bodies that move only at low speeds σ_B can be measured in a microwave anechoic chamber or on a radar scattering range. However, difficulties arise when high-velocity reentry vehicles are considered.

When a rocket or missile moves through the atmosphere at high Mach numbers, collisions of gas atoms and molecules with the vehicle surface create a shock wave around the vehicle. The high temperatures associated with the collisions will cause ionization of some of the atmospheric and ablation-product components behind the shock. The

hot gases in this plasma sheath region flow around the surface and into a long wake behind the vehicle, where recombination processes return them to neutral states. The plasma sheath and wake may strongly effect σ_B , so that the performance to be expected of a radar when it is observing a reentry vehicle can only be predicted if plasmafield interactions are considered.

A wide and diverse literature on the reentry plasma has been created by physicists, chemists and engineers working in combined research. These studies fall into four categories: (a) the basic physics of ionization and recombination processes, ¹ (b) the calculation of flow field properties, including the geometry and constituents of the sheath and wake, ² (c) analysis of the interaction between electromagnetic fields and a plasma-clad body and wake, ³ and (d) interpretation of modified radar performance and changes in data. ⁴

This communication begins (Sections II-III) with a qualitative discussion of interactions between an incident electromagnetic wave and a plasma-clad body. The purpose of these sections is to give the general reader a heuristic understanding of the problem background. Exceptions may be found to some of the behavior characteristics noted in these sections, so they should not be interpreted as being exact in every conceivable case.

In Sections IV-V, rigorous calculations of backscatter cross section have been performed for a spherical, plasmaclad body. The limitations on application of this model

The authors are with the IBM Federal Systems Division Space Systems Center in Huntsville, Alabama.

^{*} Sections I-V of this paper were supported by the Nike-X Development Office under Contract DAHC60-68-C-0019; Sections VI-VIII were supported by an IBM research program.

are presented in context with the earlier background material.

The plasma simulation technique discussed in Sections VII-VIII is a means for modeling a diverse range of reentry bodies and plasmas that are not amenable to analytic solution. As a first step, a simulated plasma can be made in the same geometry as used for the theoretical analysis of Section IV, and the theoretical data used to confirm the validity of the simulation technique. Then, in the second step, the validated technique can be used to simulate many other plasma configurations around a variety of bodies, leading to a library of data and improved ability to predict radar system performance.

II. Plasma properties

In studies of electromagnetic wave-plasma interactions, the plasma is usually described³ in terms of a complex permittivity ϵ' :

$$\epsilon' = \epsilon_0 \left[1 - \frac{\omega_p^2}{\omega^2 + g^2} - i \frac{\omega_p^2 g}{\omega(\omega^2 + g^2)} \right]$$
 (1)

In this equation ω_p is the plasma frequency defined as $[N_e e^2/m\epsilon_0]^{1/2}$, where N_e is the free electron density in the plasma, $\omega=2\pi f$ is the source frequency in radians/second, and g is the collision frequency accounting for all loss processes. If $\omega \ll \omega_p$, the imaginary part of ϵ' is large, and the plasma behaves like a metal; if $\omega \gg \omega_p$ the plasma is transparent; and if $\omega \approx \omega_p$, a critical region exists where both absorption and refraction effects may be noted.

The plasma properties may be calculated if N_e and g are known functions of position within the sheath and wake. However, aerodynamic flow field calculations are not sufficiently sophisticated to provide detailed expressions for N_e and g, and many approximations must be employed.

The radar cross section of the plasma-clad vehicle is found by considering a plane wave incident on the vehicle and solving Maxwell's equations for the scattered fields. These fields are a function of the body and plasma configuration and the plasma propagation constant K:

$$K = K_0 \sqrt{\epsilon'/\epsilon_0} = K_0(n + i\alpha), \qquad (2)$$

where K is the wave number in the plasma, $2\pi/\lambda$; K_0 is the free space wave number, $2\pi/\lambda_0$; the index of refraction $n = \text{Re } (K/K_0)$; and the absorption coefficient $\alpha = \text{Im } (K/K_0)$.

III. Radar parameters

Surveys of the literature indicate that radar performance can be directly summarized by using the range equation (Eq. 3). In order to detect the presence of an approaching missile, the scattered energy E_R received at the radar must exceed the system threshold. This energy is a function of transmitted power P_T , range R, pulse duration t_v ,

effective antenna gain G and the backscatter cross section $\sigma_B(f)$ of the missile, as given by

$$E_R = \frac{P_T G^2 t_p \sigma_B(f) \lambda^2}{(4\pi)^3 R^4}.$$
 (3)

• The plasma sheath

The plasma sheath can increase or decrease $\sigma_B(f)$ depending on whether the sheath is *underdense* (transparent), overdense (reflecting), or in the critical region (transition) at the radar frequency f. The field can penetrate the plasma to a depth of approximately $\lambda/3$, where λ , the wavelength in the plasma, can be greater or smaller than the free-space wavelength λ_0 (Eq. 2). The variation of σ_B with radar angle of observation may be strongly altered by the plasma. For example, an overdense plasma sheath tends to disguise specific features of the vehicle and smooth out the effective body surface so that σ_B is more constant with angle.

• The plasma wake

The wake will tend to strongly increase the product $t_p\sigma_B(f)$ if the wake is overdense or in the critical region and if the pulse length ct_p is long enough to include both vehicle and wake in the same range cell.*

The degree to which the wake affects the received signal may also depend on the beam width of the radar antenna. For many geometries much of the wake will lie outside the solid angle subtended by the beam. The backscatter cross section of the wake depends on whether the flow is laminar or turbulent and on the values of N_e and g; in general, the contributions to σ_B from the wake are a strong function of observing angle.

• Other plasma effects

Changes in the observation angle, reshaping of the range and angular cells and fluctuations in the plasma properties all contribute to time variations in E_R . The plasma will also change the polarization of the reflected fields and, depending on the polarization of the receiving antenna, may change the effective body cross section.

Scattering from the sheath and wake and variations in σ_B with time can all degrade the tracking accuracy of a ground radar. An analysis of the plasma-field interaction is required to determine the mean radar errors and resultant system performance. In addition, the plasma makes it more difficult to relate radar data to vehicle shape. A detailed understanding of the interaction must be obtained and included in any valid discrimination \dagger technique.

^{*} The total search or tracking range R of a radar may be divided into range cells each of the length of a transmitted pulse, ct_p . Targets within the same range cell cannot be resolved. Similarly, the angular coverage of a radar may be divided into angular cells, of width $R\theta_{beam}$, in which targets cannot be resolved.

[†] The ability to distinguish different types of vehicles by making radar measurements.

IV. Theoretical model

The simplest target model that contains the essential 3-dimensional properties inherent in the problem is a spherical conducting body surrounded by a spherical (laminar) plasma. The usefulness of this model depends on how well it represents actual reentry bodies.

The model will apply if scattering from the reentry body and sheath can be separated from wake scattering, and if the body/sheath combination can be approximated by concentric spheres.

• Separation from wake return

If $\omega_{p,\text{wake}} \ll \omega$, the wake will be transparent and will not contribute to the received fields at the radar. Since $\omega_{p,\text{sheath}}$ is larger than $\omega_{p,\text{wake}}$ this condition can hold even when sheath scattering is important.

If the wake is not transparent at the frequency of interest, the sheath and wake returns can be separated if the range cell is sufficiently short, or if the angular cell and geometry are such that the antenna beam subtends only the body and sheath.

• Body and sheath shape

If the reentry body is spherical in shape, the plasma sheath may be approximated by a concentric sphere, whose thickness and electrical properties $N_{\rm e}$, g are averages over part or all of the body surface.

At low frequencies for which the characteristic target dimensions are much less than λ (Rayleigh region), the cross section of a body depends only on its volume and not the detailed structure. In this region, the spherical model is valid for actual reentry vehicles if the radar return from the body vicinity is separable from the wake return.

At high frequencies where target dimensions are much greater than λ (optical region), scattering along the line-of-sight from radar to target is dominant since only negligible coupling exists around the body edges. The model is valid in this region for near nose-on views or if the wake return can be otherwise isolated. In this region the scattering is sensitive to fine structure of the target except when an overdense sheath shields the surface.

At resonant frequencies where the body dimensions and λ are the same order of magnitude, the field interaction is sensitive to body shape and appreciable coupling exists around the body. Within this region a significant model error may exist and care must be taken in interpreting the analysis.

V. Model analysis

Rigorous calculations have been performed by the authors for a spherical conductor surrounded by a concentric, lossy $(g \neq 0)$ spherical plasma (Fig. 1). The basic equations for this scattering are discussed by Stratton and the scat-

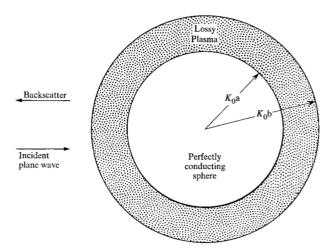


Figure 1 Geometry of the theoretical model.

tered fields are given in terms of six coefficients defined through the equations⁵

$$\begin{bmatrix} j_n(K_0b) + iy_n(K_0b) & -j_n(Kb) & -y_n(Kb) \\ \hat{j}_n(K_0b) + i\hat{y}_n(K_nb) & -\hat{j}_n(Kb) & -\hat{y}_n(Kb) \\ 0 & j_n(Ka) & y_n(Ka) \end{bmatrix} \begin{bmatrix} a_n^s \\ c_n^I \\ h_n^I \end{bmatrix} = \begin{bmatrix} -j_n(K_0b) \\ -\hat{j}_n(K_0b) \\ 0 \end{bmatrix}$$

$$\begin{bmatrix} \hat{\jmath}_{n}(K_{0}b) + i\hat{\jmath}_{n}(K_{0}b) & -\hat{\jmath}_{n}(Kb) & -\hat{\jmath}_{n}(Kb) \\ j_{n}(K_{0}b) + iy_{n}(K_{0}b) & -(K^{2}/K_{0}^{2})j_{n}(Kb) & -(K^{2}/K_{0}^{2})y_{n}(Kb) \\ 0 & \hat{\jmath}_{n}(Ka) & \hat{\jmath}_{n}(Ka) \end{bmatrix}$$

$$\begin{bmatrix} b_{n}^{s} \\ j_{n}^{I} \\ a^{I} \end{bmatrix} = \begin{bmatrix} -\hat{\jmath}_{n}(K_{0}b) \\ -j_{n}(K_{0}b) \\ 0 \end{bmatrix},$$

where $j_n(z)$ and $y_n(z)$ are spherical Bessel functions and

$$\hat{j}_n(z_1) = \left[\frac{d}{dz}(zj_n(z))\right]_{z=z_1}$$

$$\hat{y}_n(z_1) = \left[\frac{d}{dz}(zy_n(z))\right]_{z=z_1}$$

The constants a_n^I , c_n^I , f_n^I , and g_n^I determine the fields inside the plasma and the backscatter cross section σ_B is determined by the a_n^s and b_n^s coefficients through the relation

$$\sigma_B = \frac{\lambda^2}{4\pi} \left| \sum_{n=1}^{\infty} (-1)^n (2n+1) (a_n^s - b_n^s) \right|^2. \tag{4}$$

Evaluation of the coefficients is a tedious process, and calculations were performed on an IBM System 360/75. The calculations have been confirmed through analytic comparison with limiting cases and numerical comparisons with work by Murphy⁶ and Scharfman⁷ for the case of a lossless plasma.

The cross sections of some specific examples have been found numerically and the results are graphed in Figs. 2a–2f. The normalized backscatter cross section of plasmaclad spheres is plotted as a function of the thickness of the plasma sheath (in wavelengths) for given sphere diameter. The calculations have been performed for a plasma with $\omega/\omega_p \approx g/\omega_p \approx 1$, because in this critical, or transition region, the plasma properties are rapidly varying and the field interactions are difficult to predict. On the basis of the calculations, we venture the following generalizations.

For each sphere diameter, as the sheath thickness $K_0(b-a)$ increases, the cross section usually decreases at first due to absorption losses in the plasma.* Then as the sheath thickens, the larger size of the total scattering area dominates the loss per unit area, and the backscatter cross section eventually exceeds the bare-body value.

This behavior is observed in the Rayleigh region (Fig. 2a), in the optical region (Figs. 2e and 2f) and for some sphere diameters (Figs. 2b and 2d) in the resonant region.

An exception to this behavior is shown in Fig. 2c, where the return increases with a thin sheath. This is caused by the rapid oscillation in backscatter cross section with body diameter observed for bare bodies in the resonant region (Fig. 3). The thin plasma is sufficient to increase the effective body size the slight amount necessary to move from a cross section minimum (point a_1) to a maximum (point a_2).

The results of the theoretical analysis, summarized above, can be used to evaluate the proposed simulation techniques described in Sections VII-VIII. The simulation models must be able to duplicate the above effects. Once this equivalence has been confirmed, the simulation technique can be applied to a wide range of other body and plasma configurations. The theoretical and simulated data together can be used to predict and interpret actual field reentry data.

VI. Experimental techniques

At present, the most reliable method for obtaining plasma cross section information is to flight-test full-scale reentry vehicles. Gun ranges, shock tunnels and plasma jets are costly simulation techniques because the models are unrecoverable and a given test yields data for only a single point along the reentry path. All of these require a large facility with attendant problems.

Another simulation technique uses a dielectric layer on the reentry vehicle nose to simulate the reentry plasma sheath.⁸ Layers of dielectric may be removed or added to yield more-realistic in-flight information. Unfortunately the dielectric only poorly simulates the plasma properties.†

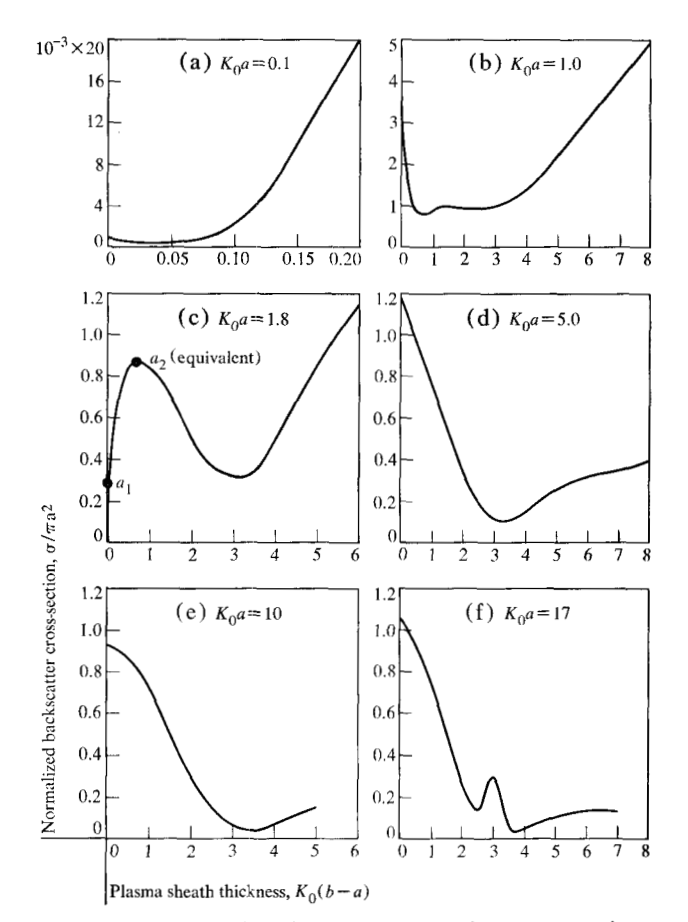
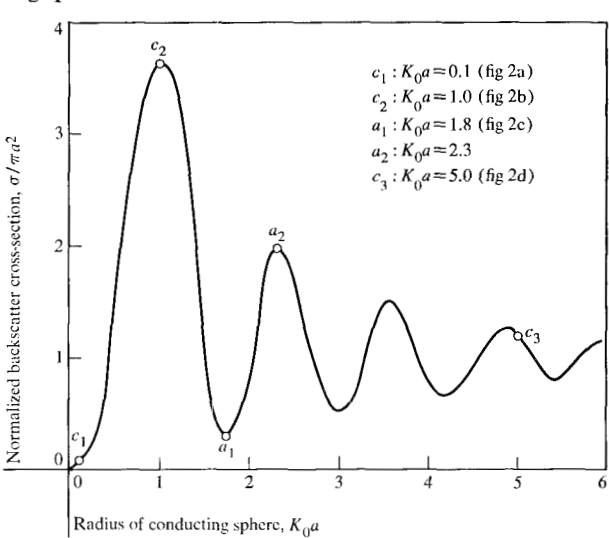


Figure 2 Normalized backscatter cross section as a function of plasma thickness. (a) $K_0a = 0.1$; (b) $K_0a = 1.0$; (c) $K_0a = 1.8$; (d) $K_0a = 5.0$; (e) $K_0a = 10.0$; and (f) $K_0a = 17.0$. For all curves, n = 0.7 and $\alpha = 0.3$.

Figure 3 Normalized backscatter cross section of a conducting sphere.



^{*} This decrease in σ_B due to absorption varies only slowly with frequency and is noted in all three scattering categories. The decrease in σ_B calculated by Murphy⁶ for a lossless plasma is due to resonant-region interference, and is sharply frequency dependent.

[†] The dielectric has reasonable collision frequencies for plasma simulation, but the numerical value of electron density is much too low (See Section VII).

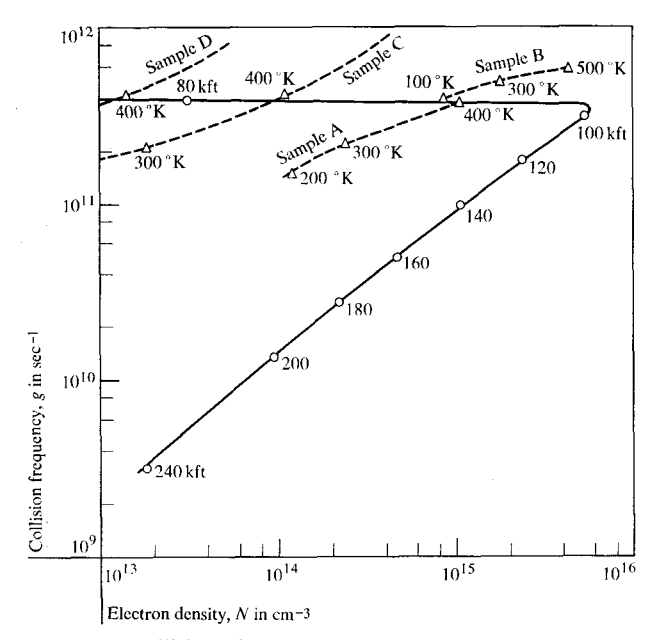


Figure 4 Collision frequency as a function of electron density (after Drummond⁹). The dashed lines show how varying the temperature of semiconductors with different properties can simulate the electromagnetic properties of plasma over given ranges of altitude.

It would be advantageous to have a reentry model with the advantages of the gun range, i.e., realistic plasma values; yet with the permanence and flexibility of a solid simulation material. The next sections contain a theoretical analysis of such a simulation technique. The experimental verification of the method can be accomplished in an inexpensive facility, by using a spherical model and comparing measured data with the theoretical results in Section V.

VII. Simulation materials

The optical parameters n and α of a plasma are completely determined by the electron density N (via the plasma frequency) and the collision frequency. The electromagnetic field intensity in the plasma caused by a ground radar is always sufficiently small to eliminate nonlinear effects. The optical properties of virtually any pure solid material, whether conductor, semiconductor, or dielectric, are similarly determined (for microwave frequencies) by the free carrier density and collision frequency of the carriers in the material. The simulation problem is reduced to finding a solid whose free electron densities and collision frequencies correspond to the plasma electron densities and collision frequencies for a typical reentry vehicle plasma sheath.

A plot of plasma electron density vs. collision frequency for a typical reentry vehicle⁹ is shown in Fig. 4. Figure 5

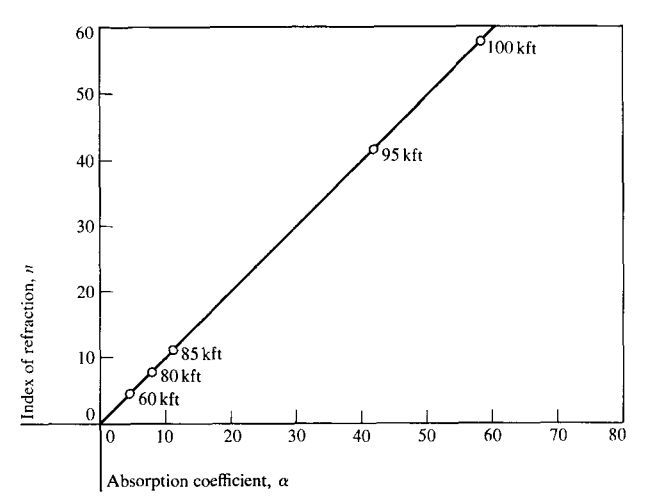


Figure 5 Index of refraction as a function of absorption coefficient, where each point on the curve corresponds to a different altitude.

shows the range of n and α for these conditions. The range of altitudes covered is 80,000 to 180,000 ft, those pertinent for terminal defense systems. Throughout this range it is observed that collision frequencies of the order of $10^{11} \, \mathrm{sec}^{-1}$ are observed, with electron densities ranging between 10^{13} and $10^{16} \, \mathrm{cm}^{-3}$. (Because of the narrowness of the reentry corridor, data for other reentry vehicles does not differ appreciably from that shown in Fig. 4.) A suitable simulation material should thus be one for which the following requirements are satisfied:

- 1. Electron conduction should dominate (hole contribution to the conductivity is negligible).
- 2. The material should be isotropic.
- 3. The free electron-densities should be in the range $10^{13} \le N \le 10^{16}$, and ideally, be variable with temperature over this range.
- 4. The collision frequency should be approximately 10^{11} sec^{-1} .

The free-electron densities and collision frequencies of conductors and (predominantly n-type) semiconductors may be related to their conductivity, σ , and Hall coefficient, R_H , by

$$N = \frac{1}{eR_H}$$

$$g = \frac{Ne^2}{m^*\sigma} ,$$

where m^* is the "effective" mass of the conduction electrons. If R_H is measured in cm³ coul⁻¹ and σ in ohm⁻¹ cm⁻¹, then N in cm⁻³ and g in sec⁻¹ are given by

$$N = \frac{6.36 \times 10^{18}}{R_H}$$

$$g = \frac{2.34 \times 10^{15}}{\sigma R_H} \frac{m}{m^*}.$$

For a typical conductor at room temperature, $\sigma = 5 \times 10^5 \text{ ohm}^{-1} \text{ cm}^{-1}$, $R_H = 10^{-4} \text{ cm}^3 \text{ coul}^{-1} \text{ and } m^* = m$, which gives $g \approx 10^{13} \text{ sec}^{-1}$, $N \approx 10^{22} \text{ cm}^{-3}$. Although g may be brought close to the required value by going to very low temperatures ¹⁰ (below 100°K), such a procedure would be quite expensive.

An alternative that immediately suggests itself is the utilization of semiconducting III-V compounds, noted for their high mobility ($\mu = \sigma R_H$) values and correspondingly lower collision frequencies. The highest mobility compound of this group is indium antimonide, which has a mobility of 77,000 cm² volt⁻¹ sec⁻¹ at room temperature. Hole mobility is low enough for electron motion to dominate. In spite of the rather unfavorably low effective mass, $m^* = 0.013m$, this compound has a collision frequency of 2.3 \times 10¹² sec⁻¹ and an electron density of 2.1 \times 10¹⁶ cm⁻³ at room temperature. At 100°K, the corresponding values are $g = 1.7 \times 10^{12}$ sec⁻¹ and $N = 6.7 \times 10^{13}$ cm⁻³. The latter values may be brought into the required neighborhood by frequency scaling.

The radar scattering cross section of the true reentry vehicle at L-band may be found from the pattern measured for a model at X-band. Scaling of the frequency by a factor of 10 will reduce the effective g by a factor of 10, while reducing the apparent N by a factor of 100. Thus, at room temperature, an InSb sample should be characterized by a collision frequency of $g_A = 2.3 \times 10^{11} \text{ sec}^{-1}$ and an electron density of $N_A = 2.1 \times 10^{14} \text{ cm}^{-3}$, where N_A and N_A are the "apparent" values of these parameters for N_A -band radiation; i.e., the complex propagation constant at N_A -band for a material with properties N_A at N_A at N_A at N_A at N_A at N_A and N_A at N_A

Approximate values of N_A versus g_A for three different samples are shown in Fig. 4. Sample C is an intrinsic sample of high purity, while samples A and B are doped (n-type) samples with impurity concentrations of 1.3 \times 10^{16} cm⁻³ and 1.0×10^{17} cm⁻³. Tor each sample, the effect of increasing the temperature is to increase the free electron density, and to gradually increase the collision frequency. The electromagnetic properties of the reentry plasma over a range of altitudes may be approximately modeled by choosing an appropriate semiconductor sample; N and g are varied over the given range by changing the temperature of the sample.

VIII. Application notes

An apparent obstacle to the use of such semiconductors for the plasma simulation problem is the anisotropy of some crystalline materials. However, it should be possible to surmount this by constructing a moulage of semicon-

ducting particles embedded in a dielectric medium. If the particles are randomly oriented, the effect of any anisotropy of the medium on the fields will be eliminated. If the percentage by volume of dielectric is small and the semiconductor particle size is smaller than the wavelength, λ , of the radiation but larger than the amplitude, X_m , of the electron oscillations, the observed electron density and collision frequency will be those characteristic of the semiconductor.* Furthermore, increasing the volume of dielectric should decrease the effective electron density by the ratio of the semiconductor volume to the total volume, while the collision frequency remains at the value characteristic of the semiconductor, provided the restrictions noted on particle size are observed. Curve D in Fig. 4 shows the behavior of the intrinsic material, Sample C, mixed in a 10:1 volume ratio.

An alternative simulation material would be a conductor-dielectric moulage at very low temperatures (below 100° K) with scaling, which yields apparent values of g_A and N_A in the same range. As previously noted, such a procedure may be ruled out for economic reasons unless unforeseen difficulties arise with the InSb simulation.

IX. Conclusions

A spherical model has been used to calculate the back-scatter cross section of a plasma-clad sphere as a function of the normalized plasma thickness. In certain circumstances the physical interpretation of this analysis allows one to predict, at least qualitatively, the plasma effects that will be observed during field radar measurements. However, in order to accurately predict the plasma effects associated with a wide variety of reentry conditions, mathematical techniques must be supplemented by various modeling techniques.

Gun ranges, shock tubes and actual field tests are expensive and time-consuming, so that suitable simulation techniques are needed. The method that has been described above appears to be a feasible means for obtaining useful laboratory data. It will now be necessary to check the model's adequacy. This can be done by directly comparing results obtained through simulation with the curves computed for the spherical model. If the comparison is good, a wide range of plasma effects may be simulated by varying the temperature of an appropriately doped semiconductor which coats a conducting body of arbitrary size and shape.

X. References

 For example, H. R. Griem, Plasma Spectroscopy, Mc-Graw-Hill Book Co., New York, 1964.

^{*} For a typical simulation using a wavelength of 10^{-2} m and a one-watt transmitter, the maximum electric field strength at 10 m from the source is of the order of 1V/m, which gives a maximum displacement of 10^{-10} m, and the semiconductor particle size should be held between 10^{-10} and 10^{-2} m.

- 2. For a recent summary, see "Minutes on the Discussion of Communication Through the Reentry Plasma Sheath (Part II)," Ohio State University Electro Science Laboratory, Technical Report 2438-2, October 1967.
- 3. For example, V. L. Ginzberg, Properties of Electromagnetic Waves In Plasma, Gordon and Breach, 1961.
- 4. See bibliography in "Special Issue on Radar Reflectivity," *Proceedings of the IEEE* 53, (August 1965).
- J. A. Stratton, Electromagnetic Theory, McGraw-Hill Book Co., New York, 1941.
- E. L. Murphy, "Reduction of Electromagnetic Backscatter From a Plasma-Clad Conducting Body," *Journal of Applied Physics* 36, 1918–27, (June 1965).
- 7. H. Scharfman, "Scattering From Dielectric Coated Spheres in the Region of the First Resonance," *Journal of Applied Physics* 25, 1352-56 (November 1954).

- E. L. Murphy, MTT Lincoln Laboratory Technical Report #294, 17 January 1963.
- J. E. Drummond, "Radio Propagation in Reentry Plasmas," Conference on the Applications of Plasma Studies to Reentry Vehicle Communications (Vol. I), October 1967.
- 10. For low-temperature dependence of conductor properties, see Condon & Odishaw, *Handbook of Physics*.
- 11. From O. Madelung, *Physics of III—V Compounds*, John Wiley and Sons, New York, 1964.
- 12. Ibid.
- 13. The dependence is of approximately $T^{s/2}$ for the temperature range in question; see Ref. 10.

Received January 10, 1969